# Reduced charge state of MeV carbon cluster constituents exiting thin carbon foils

A. Brunelle, S. Della-Negra, J. Depauw, D. Jacquet, Y. Le Beyec, and M. Pautrat
*Institut de Physique Nucléaire, CNRS-IN2P3, F-91406 Orsay Cedex, France*
(Received 22 December 1998)

Direct determination of average charge states have been performed with an electrostatic analysis method for carbon ions and carbon cluster ($C_n$, $n=3-10$) constituents exiting thin carbon foils. The velocity of the mono and polyatomic projectiles was identical, ranging from 1–4 MeV per atom. The average charge state of carbon cluster constituents is significantly reduced as compared to that of a single carbon projectile at the same velocity, the larger the size of the cluster, the smaller the charge state per cluster atom. This lowering effect decreases when the foil thickness increases. [S1050-2947(99)08606-0]

PACS number(s): 34.50.Dy, 34.50.Fa, 36.40.Wa

## I. INTRODUCTION

The passage of swift MeV polyatomic ions through thin solid films has been studied for many years. Small molecular ions and hydrogen clusters were mainly used as projectiles in the early experiments, which were mostly focused on energy-loss measurements [1–6]. Recently, it has been possible to produce and accelerate large-size clusters over a considerable range of velocities in the regimes of nuclear and electronic stopping.

When a fast cluster penetrates a solid, the binding electrons are stripped away and the charged-cluster constituents, spatially and temporally correlated, tend to separate due to their mutual Coulomb repulsion. Several authors have reported that by comparison with single atoms passing through thin foils, the average charge state of the constituents of polyatomic projectiles is lower than the charge of an individual atom [7–13]. An enhanced electron-capture probability at the foil exit, which depends on the internuclear separation distance between the fragment constituents, was proposed by Maor *et al.* [7]. Electron-capture processes have been reported in foil-induced dissociation of small molecular ions as $OH^+$ and $CH^+$ [8–10]. The passage of hydrogen clusters $H_n$ (with $n \leqslant 21$) through a solid target was studied by the Lyon group [11,12]. The final charge state (per atom) is supposed to depend on the ''volume'' occupied by the cluster atoms at the exit side of the foil [12]. Vicinage effects are of considerable importance for explaining the lowering of the average charge states of cluster-atomic constituents and an enhanced electron-capture model for closely spaced ions has also been presented by Steuer and Richtie [13]. For large size and mass clusters there is no result on charge-state measurements of atomic cluster constituents exiting solid foils. In the present paper we focus on carbon clusters $C_n$ ($n=3-10$) at energies from 1–4 MeV per atom passing through thin amorphous carbon foils. The average charge states of the exiting carbon constituents were measured directly and compared to the charge state of single-carbon projectiles at the same velocity. Carbon foils with different thicknesses were used and all the measurements were performed under the same experimental conditions.

## II. EXPERIMENT

Carbon clusters were accelerated by the 15-MV tandem accelerator at IPN, Orsay. In a standard sputtering Cs ion source, $Cs^+$ ions of 20 keV bombard a graphite target. Negative cluster ions of $C_n^-$ are extracted, accelerated, and mass selected before being injected in the tandem accelerator [14]. At the high-voltage terminal, the $C_n^-$ clusters collide with $N_2$ molecules in the gas stripper channel and become positively charged. The beam can be pulsed at the low-energy side; therefore, after full acceleration, positive $C_n^+$ cluster ions are identified by time-of-flight measurements and also by magnetic deflection and energy measurements. We have used beams of $C_3^+$, $C_5^+$, $C_8^+$, and $C_{10}^+$ at almost the same energy per atom (same velocity) by adjustment of the terminal voltage.

The experimental set up is shown in Fig. 1. Upstream of the target foil the size of the cluster beam is defined by vertical and horizontal slits which, in the present experiment, had a 0.3-mm aperture in both directions. At 40 cm behind the slits four carbon foils with different thicknesses are fixed on a target holder. When a cluster projectile hits the entrance face of the target, electrons are emitted, accelerated by a few hundred volts in the direction opposite to the beam, electrostatically deflected at 90° and detected by a set of dual microchannel plates. A time signal corresponding to the passage of the cluster in the carbon foil is generated and used to trigger the experiment. Since very thin carbon foils may have pinholes, the electron detection ensures that the projectile did not pass through holes but through the foil.[1] Two parallel and horizontal deflection plates (length = 60 mm, distance between plates = 10 mm) are placed 5 mm after the target. Voltage values of $\pm 3$ kV to $\pm 15$ kV can be applied on each deflection plate. After passing through the foils, the exiting fragments of carbon atoms are multiply charged. The measurements of the deviation after the deflection plates along the deflection axis allows calculation of the charge states.

For this purpose a multi-impact position sensitive detector is located at 32 cm from the center of the deflection plates. This original detector and its dedicated electronics have been

[1]The carbon foils were manufactured by ACF Metals (Tucson, Arizona), and their thicknesses were measured at Orsay (with an accuracy of less than 10%) by the Rutherford backscattering technique with 1.2-MeV $^4$He particles. The thickness of the foils used in this experiment was ranging from 2.2 $\mu$g/cm$^2$ up to 40 $\mu$g/cm$^2$.

 

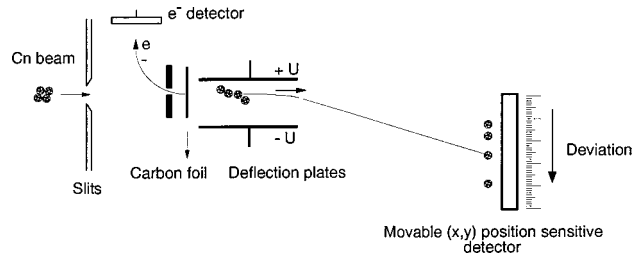


FIG. 1. Experimental setup.

built and tested at IPN [15,16] . The detector consists of two channel plates of 45 mm in diameter with an ''anode'' made of 256 discrete anodes ($16\times16$). These anodes, drawn with a step size of 2.54 mm are shielded by a thin grid (0.12-mm wires) connected to the ground. There are rigid and very short connections from the 256 anodes to 16 electronic boards, each of them containing 16 circuits with threshold discriminators. The time signals are transported through special ribbon cables to 4 electronic boards for time measurements, with 64 input each. Each of these 64 pixels boards contains 8 time to digital converters (TDC) [16]. The main characteristics of one TDC are the following: 8 completely independent stop signal inputs associated with one start signal, time bin 0.225 ns, dead time 20 ns, time range up to several ms. There is also a possibility not used in the present paper to encode the analogic signals issued from the 256 anodes.

The response of the detector was checked with focused and pulsed beams of gold ions at 20 keV produced by a liquid metal ion source and also with small-size beams of $C_1$ (0.3 mm$\times$0.3 mm) at 1 MeV. The cross talk between two adjacent pixels is less than $10^{-4}$ and the efficiency of electron collection is better than 90%. The multi-impact position sensitive detector (MIPSD) can be mechanically moved precisely in the vertical and horizontal direction in a plane perpendicular to the beam axis.

A careful calibration of the electrostatic deviation of the deflection plates was achieved with a (0.3-mm$\times$0.3-mm) collimated $C_1^+$ beam. First the detector position was precisely adjusted, in such a way that the incident beam hits the detector exactly in the middle of an interpixel region for no deflection voltage. This position corresponds to an equivalent counting rate on the two adjacent pixels. Then, different deflection voltages were applied ($\pm5$ kV, $\pm8$ kV), leading to a displacement of the beam spot on the detector. The position of the fired pixel (giving the number of 2.54-mm steps of the deviation) is noted and the fine determination of this displacement is then achieved by moving the detector in the vertical direction until a new interpixel wire is found exactly in the middle of the deflected $C_1^+$ ions spot. The impact of the $C_1^+$ beam corresponding to the interpixel position can be defined with an accuracy better than 100 $\mu$m [15]. The deviation distances determined as the sum of this fine displacement and the 2.54-mm steps number are used for the calibration. For the cluster constituents, the influence of the Coulomb explosion cone on the average trajectories (which leads at the most to a relative variation of the deviation distance smaller than $10^{-3}$) has been neglected. In this experiment where the deflection voltage was set to ensure a complete detection of the charge distribution in the detector, the spatial resolution of the MIPSD is too low to separate completely each charge state. However, average values and standard deviations of the measured charge-state distributions have been extracted with rather low statistical uncertainties.

## III. EXPERIMENT RESULTS AND DISCUSSION

Average charge-state values of carbon ions at incident energies close to 1, 2, and 4 MeV passing through carbon foils with various thicknesses are given in Table I. In this energy range, due to the high-ionization cross sections for carbon ions ($\sigma\geqslant10^{-16}$ cm$^2$ [17]), the required traveling distance in the target to reach equilibrium is close to 1 nm. The $C_1$ charge state values reported in Table I are thus equilibrium charge states, which are in good agreement with previous experimental results [18]. A summary of the average charge states of $C_1$ projectiles at various energies, behind carbon foils, is given in Ref. [19].

Different cluster beams ($C_3^+$ to $C_{10}^+$) at incident energies per atom close to 2 MeV for $C_3^+$ and $C_8^+$, 1 and 2 MeV for $C_{10}^+$, and 1, 2, and 4 MeV for $C_5^+$ were passing through the same carbon foils as $C_1$. For each projectile the exit energies (see column 3 in Table I) have been calculated with the TRIM code, neglecting small difference of energy loss for single atoms and $C_n$ constituents [20] . The average charge states per atom $\langle q_n\rangle$ corresponding to the different incident carbon clusters $C_n$ are given in Table I. The uncertainties reported in Table I take into account the statistical uncertainties on the centroid determination as well as experimental uncertainties on beam energies, deflection voltage, and a possible contamination (less than 10%) of fragmented incident clusters resulting from interaction with residual gas molecules.

For all cluster projectiles used in this experiment, the average charge states of the exiting constituents are smaller than the charge state of the single carbon atom at the same velocity. The variation of the cluster constituent charge ratio $\langle q_n\rangle/\langle q_1\rangle$, at a given velocity, as a function of the target thickness is shown in Fig. 2 for the 2-MeV/atom data: a continuous increase of this charge ratio with the foil thickness is observed. For thin targets the $\langle q_n\rangle$ values differ considerably from the average charge $\langle q_1\rangle$ of $C_1$ traveling with the same velocity. The difference is more pronounced when the number of atoms in the incident clusters increases as shown in Fig. 3 for $C_n$ ($n=3,5,8,10$) passing through a 2.2-$\mu$g/cm$^2$ carbon foil. On this figure is also reported the charge ratio from Ref. [7] for molecular nitrogen ions accelerated at 2.1 MeV/atom, exiting a 100-Å carbon foil. This $N_2$ result is in very good agreement with the evolution with the number of projectile constituents that can be extracted from our measurements.

The charge ratio approaches slowly the unit value for thicker targets. This evolution reflects the increase of the traveling interconstituent distance due to Coulomb explosion and multiple scattering on the target atoms.

However, for the thin foils used in these experiments, the $C_n$ fragment ions at energies of 1–4 MeV/atom do not separate very much from each other at the foil exit. For example, it can be estimated that for 10-MeV $C_5$ clusters the mean radial distance between ions are close to 2 Å at the exit of a

TABLE I. Average charge states per atom measured for the different carbon cluster projectiles exiting various carbon foils.

| Projectile | Incident energy[a] per atom | Foil thickness[b] | Exit energy[a] per atom | Average charge state per atom |
|---|---|---|---|---|
| | 3.81 | 5.30 | 3.77 | 3.60 ± 0.06 |
| | 3.81 | 10.20 | 3.73 | 3.72 ± 0.05 |
| | 3.81 | 15.00 | 3.69 | 3.68 ± 0.05 |
| | 3.81 | 40.00 | 3.52 | 3.63 ± 0.08 |
| | 1.92 | 2.20 | 1.90 | 2.84 ± 0.04 |
| | 1.92 | 3.40 | 1.89 | 2.85 ± 0.04 |
| C1 | 1.92 | 5.30 | 1.88 | 2.84 ± 0.04 |
| | 1.92 | 10.20 | 1.84 | 2.84 ± 0.04 |
| | 1.92 | 15.00 | 1.81 | 2.82 ± 0.04 |
| | 1.92 | 40.00 | 1.63 | 2.68 ± 0.09 |
| | 0.96 | 5.30 | 0.93 | 1.98 ± 0.04 |
| | 0.96 | 10.20 | 0.89 | 1.90 ± 0.03 |
| | 0.96 | 15.00 | 0.85 | 1.88 ± 0.04 |
| | 0.96 | 40.00 | 0.67 | 1.61 ± 0.05 |
| | 2.00 | 2.20 | 1.98 | 2.10 ± 0.04 |
| | 2.00 | 3.40 | 1.97 | 2.11 ± 0.04 |
| | 2.00 | 5.30 | 1.96 | 2.16 ± 0.04 |
| | 2.00 | 5.30 | 1.96 | 2.28 ± 0.07 |
| | 1.98 | 5.30 | 1.94 | 2.30 ± 0.04 |
| C10 | 1.98 | 10.20 | 1.90 | 2.45 ± 0.07 |
| | 1.98 | 15.00 | 1.87 | 2.52 ± 0.07 |
| | 1.98 | 40.00 | 1.69 | 2.52 ± 0.11 |
| | 0.99 | 2.20 | 0.97 | 1.69 ± 0.04 |
| | 0.99 | 5.30 | 0.95 | 1.71 ± 0.04 |
| | 1.97 | 2.20 | 1.96 | 2.25 ± 0.06 |
| | 1.97 | 3.40 | 1.95 | 2.27 ± 0.06 |
| C8 | 1.97 | 5.30 | 1.93 | 2.33 ± 0.06 |
| | 1.97 | 10.20 | 1.90 | 2.48 ± 0.06 |
| | 1.97 | 15.00 | 1.86 | 2.54 ± 0.06 |
| | 1.97 | 40.00 | 1.68 | 2.53 ± 0.11 |
| | 3.99 | 5.30 | 3.95 | 3.16 ± 0.08 |
| | 3.99 | 10.20 | 3.92 | 3.35 ± 0.08 |
| | 3.99 | 15.00 | 3.88 | 3.44 ± 0.08 |
| | 3.99 | 40.00 | 3.70 | 3.54 ± 0.12 |
| | 2.01 | 5.30 | 1.97 | 2.46 ± 0.06 |
| C5 | 2.01 | 15.00 | 1.90 | 2.53 ± 0.06 |
| | 2.01 | 40.00 | 1.72 | 2.60 ± 0.08 |
| | 1.97 | 2.20 | 1.95 | 2.34 ± 0.06 |
| | 1.97 | 3.40 | 1.94 | 2.37 ± 0.06 |
| | 1.97 | 5.30 | 1.93 | 2.42 ± 0.07 |
| | 1.02 | 5.30 | 0.98 | 1.81 ± 0.05 |
| | 1.02 | 10.20 | 0.94 | 1.82 ± 0.05 |
| | 1.02 | 15.00 | 0.91 | 1.79 ± 0.05 |
| | 1.02 | 40.00 | 0.73 | 1.59 ± 0.06 |
| | 1.96 | 2.20 | 1.95 | 2.49 ± 0.07 |
| | 1.96 | 3.40 | 1.94 | 2.53 ± 0.07 |
| C3 | 1.96 | 5.30 | 1.92 | 2.56 ± 0.05 |
| | 1.96 | 10.20 | 1.89 | 2.66 ± 0.07 |
| | 1.96 | 15.00 | 1.85 | 2.69 ± 0.07 |
| | 1.96 | 40.00 | 1.67 | 2.63 ± 0.11 |

[a]The energies per atom are given in MeV/atom.

[b]The foil thickness is given in $\mu g/cm^2$.

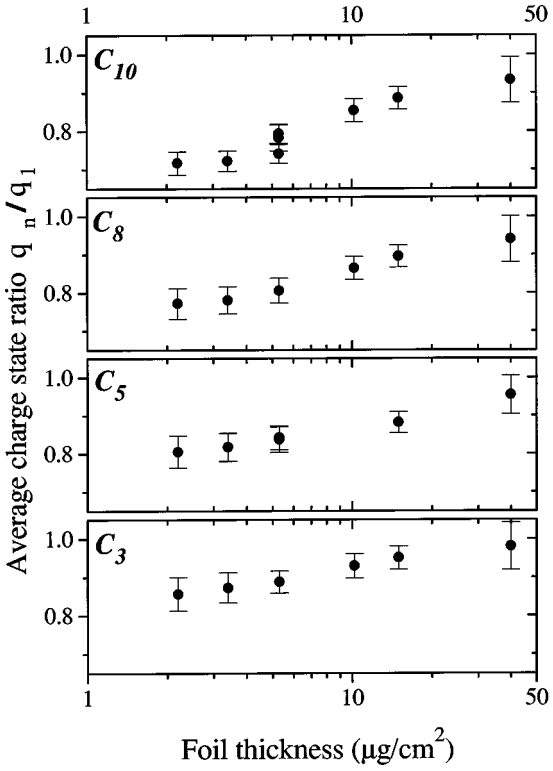


FIG. 2. Average charge-state ratio $\langle q_n \rangle / \langle q_1 \rangle$ (see text) measured for the different carbon cluster projectiles impinging at about 2-MeV/atom different carbon foils, plotted as a function of the foil thickness given in $\mu$g/cm$^2$.

6-$\mu$g/cm$^2$ foil [21]. This estimate includes multiple scattering and unshielded Coulomb explosion. The ion-ion proximity of the cluster constituents can, therefore, modify the charge-changing processes. Figure 3 shows that the influence of this proximity is a monotonous function of the number of projectile constituents, regardless of the cluster structure. (For example, $C_3^+$ has a closed structure [22] whereas $C_5^+$ is linear [23]. The average number of closest neighbors is thus larger in $C_3^+$ than in $C_5^+$, nevertheless the proximity effect is larger for the $C_5^+$ projectile).

The neighbor constituents create a perturbation of the atomic potential, which would result in a stronger binding of remaining electrons. A simple approach is to consider an average shift $\Delta I$ of the atomic levels that depends on the nuclear distance and only slightly on the initial shape of the cluster [12]. The ionization of the cluster constituents may be more difficult due to the apparent increase of the electron-binding energy during the passage through the solid. The electron capture may be also modified by this additional potential $\Delta I$ that results of the vicinage effects of the multiply charged carbon atoms. Inside targets, screening effects may reduce the $\Delta I$ potential while at the exit of the solid the vanishing of screening effects would enhance the electron-capture probability. The mean charge state per atom, which is measured at the exit side, would therefore be lower than the charge state inside.

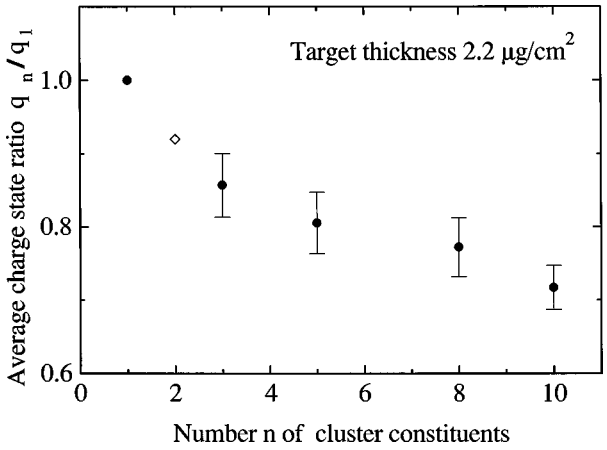


FIG. 3. Evolution with the number $n$ of cluster constituents of the charge ratio $\langle q_n \rangle / \langle q_1 \rangle$, measured at the exit of a 2.2 $\mu$g/cm$^2$ carbon foil, for 2-MeV/atom carbon cluster projectiles. The diamond symbol shows data extracted from Ref. [7] for 2.1-MeV/atom $N_2$ projectiles.

This additional potential can be written as $\Delta I \propto \Sigma_{i,j} q_i \cdot q_j / r_{ij}$ where the sum extends to all cluster constituents of charge $q_{i,j}$ and where $r_{ij}$ is the relative distance between pairs of ions. Since the interconstituent distance increases relatively slowly with the target thickness, the magnitude of this potential could still be of the order of several eV for 100-nm thick targets, and thus it would be still effective for such large thicknesses as observed experimentally.

## IV. CONCLUSION

Mean values of charge-state distributions after thin carbon foils have been measured for single carbon atoms and large-size carbon cluster projectiles ($C_n$, $n=3$ to 10) between 1–4 MeV per atom. The average charge state of carbon cluster constituents is significantly reduced as compared to that of a single carbon projectile at the same velocity. The average charge state per atom decreases continuously when the number of constituents increases. For a given projectile, the interconstituent mean distance increases with the foil thickness and, therefore, the charge reduction (due to the constituent proximity) progressively vanishes.

## ACKNOWLEDGMENTS

We gratefully acknowledge G. Maynard and T. Tombrello for fruitful discussions. We are also very grateful to R. Sellem, P. Cohen, and J. Le Bris for their invaluable help during the design and the tests of the MIPSD.

[1] W. Brandt, A. Ratkowski, and R.H. Ritchie, Phys. Rev. Lett. **33**, 1325 (1974).

[2] Z. Vager and D. Gemmel, Phys. Rev. Lett. **37**, 1352 (1976).

[3] J.W. Tape, W.M. Gibson, J. Rémillieux, R. Laubert, and H.E. Wegner, Nucl. Instrum. Methods **132**, 5 (1976).

[4] W. Brandt and R.H. Ritchie, Nucl. Instrum. Methods **132**, 43 (1976).

[5] R. Levi-Setti, K. Lam, and T.R. Fox, Nucl. Instrum. Methods **194**, 281 (1982); M.F. Steuer, D.S. Gemmel, E.P. Kanter, E.A. Johnson, and B.J. Zabransky, *ibid.* **194**, 277 (1982).

[6] A. Clouvas, M.J. Gaillard, A.G. de Pinho, J.C. Poizat, J. Rémillieux, and J. Desesquelles, Nucl. Instrum. Methods Phys. Res. B **2**, 273 (1984); D. Gemmel, J. Rémillieux, J.C. Poizat, M.J. Gaillard, R.E. Holland, and Z. Vager, Nucl. Instrum. Methods **132**, 6167 (1976).

[7] D. Maor, P.J. Cooney, A. Faibis, E.P. Kanter, W. Koenig, and B.J. Zabransky, Phys. Rev. A **32**, 105 (1985).

[8] A. Faibis, G. Goldring, M. Hass, R. Kaim, I. Plesser, and Z. Vager, Nucl. Instrum. Methods **194**, 299 (1982).

[9] A. Breskin, A. Faibis, G. Goldring, M. Hass, R. Kaim, Z. Vager, and N. Zwang, Phys. Rev. Lett. **42**, 369 (1979).

[10] I. Plesser, E.P. Kanter, and Z. Vager, Phys. Rev. A **29**, 1103 (1984).

[11] M.J. Gaillard, J.C. Poizat, A. Ratkowski, and J. Rémillieux, Nucl. Instrum. Methods **132**, 69 (1976).

[12] B. Mazuy, A. Belkacem, M. Chevallier, M.J. Gaillard, J.C. Poizat, and J. Rémillieux, Nucl. Instrum. Methods Phys. Res. B **28**, 497 (1987); **33**, 105 (1988).

[13] M.F. Steuer and R.H. Ritchie, Nucl. Instrum. Methods Phys. Res. B **40/41**, 372 (1989).

[14] Ch. Schoppmann, P. Wohlfart, D. Brandl, M. Sauer, Ch. Tomaschko, H. Voit, K. Boussofiane, A. Brunelle, P. Chaurand, J. Depauw, S. Della-Negra, P. Håkansson, and Y. Le Beyec, Nucl. Instrum. Methods Phys. Res. B **82**, 156 (1993); S. Della-Negra, A. Brunelle, Y. Le Beyec, J.M. Curaudeau, J.P. Mouffron, B. Waast, P. Håkansson, B.U.R. Sundqvist, and E. Parilis, *ibid.* **74**, 453 (1993); K. Boussofiane-Baudin, A. Brunelle, P. Chaurand, J. Depauw, S. Della-Negra, P. Håkansson, and Y. Le Beyec, Int. J. Mass Spectrom. Ion Processes **130**, 73 (1994).

[15] S. Della-Negra, D. Jacquet, P. Cohen, J. Depauw, R. Douet, S. Du, J. Le Bris, and R. Sellem, IPN Technical Biannual Report No. 72, 1994-1995 (unpublished); S. Della-Negra *et al.* (unpublished).

[16] R. Sellem, IPN Technical Biannual Report No. 79, 1994-1995 (unpublished).

[17] A.S. Schlachter, J.W. Stearns, W.G. Graham, K.H. Berkner, R.V. Pyle, and J.A. Tanis, Phys. Rev. A **27**, 3372 (1983).

[18] Ch. Stoller, M. Suter, H. Himmel, G. Bonani, M. Nessi, and W. Wlfli, IEEE Trans. Nucl. Sci. **NS-30**, 1074 (1983).

[19] K. Shima, N. Kuno, M. Yamanouchi, and H. Tawara, At. Data Nucl. Data Tables **51**, 173 (1992).

[20] K. Baudin, A. Brunelle, M. Chabot, S. Della Negra, J. Depauw, D. Gardes, P. Håkanson, Y. Le Beyec, A. Billebaud, M. Fallavier, J. Rémillieux, J.C. Poizat, and J.P. Thomas, Nucl. Instrum. Methods Phys. Res. B **94**, 341 (1994).

[21] J. Hartmann, Ph.D. thesis, Caltech, 1997 (unpublished).

[22] A. Faibis, E.P. Kanter, L.M. Tack, E. Bakke, and B.J. Zabransky, J. Phys. Chem. **91**, 6445 (1987).

[23] W.J. Weltner and R. J. Von Zee, Chem. Rev. **89**, 1713 (1989).